ANNUAL REVIEWS

Annual Review of Physiology

Mechanisms Underlying Calcium Nephrolithiasis

R.T. Alexander,[1,2] D.G. Fuster,[3] and H. Dimke[4,5]

[1]Departments of Physiology and Pediatrics, University of Alberta, Edmonton, Canada; email: todd2@ualberta.ca

[2]Membrane Protein Disease Research Group, University of Alberta, Edmonton, Canada

[3]Department of Nephrology and Hypertension, Inselspital, Bern University Hospital, University of Bern, Bern, Switzerland

[4]Department of Cardiovascular and Renal Research, Institute of Molecular Medicine, University of Southern Denmark, Odense, Denmark

[5]Department of Nephrology, Odense University Hospital, Odense, Denmark

Annu. Rev. Physiol. 2022. 84:559–83

First published as a Review in Advance on October 26, 2021

The *Annual Review of Physiology* is online at physiol.annualreviews.org

https://doi.org/10.1146/annurev-physiol-052521-121822

Keywords

kidney stones, hypercalciuria, epithelial transport

Abstract

Nephrolithiasis is a worldwide problem with increasing prevalence, enormous costs, and significant morbidity. Calcium-containing kidney stones are by far the most common kidney stones encountered in clinical practice, and thus, hypercalciuria is the greatest risk factor for kidney stone formation. Hypercalciuria can result from enhanced intestinal absorption, increased bone resorption, or altered renal tubular transport. Kidney stone formation is complex and driven by high concentrations of calcium-oxalate or calcium-phosphate in the urine. After discussing the mechanism mediating renal calcium salt precipitation, we review recent discoveries in renal tubular calcium transport from the proximal tubule, thick ascending limb, and distal convolution. Furthermore, we address how calcium is absorbed from the intestine and mobilized from bone. The effect of acidosis on bone calcium resorption and urinary calcium excretion is also considered. Although recent discoveries provide insight into these processes, much remains to be understood in order to provide improved therapies for hypercalciuria and prevent kidney stone formation.

INTRODUCTION

Kidney stones are a common, costly condition, with nearly 11% of American men and 7% of women reporting having had a kidney stone at least once (1). Recurrence risk is high, and treatment of kidney stones costs more than 2 billion dollars annually in the United States alone (1, 2). Kidney stone formation is associated with other common metabolic diseases, including obesity, diabetes, inflammatory bowel disease, and hypertension (3–6). Further, people with kidney stones are at an increased risk of adverse health outcomes such as kidney and cardiovascular disease (3, 4, 7, 8). Thus, understanding the risk factors contributing to kidney stone formation is important for prevention and cost reduction.

Most kidney stones are composed of calcium (~85%), complexed to either oxalate or phosphate (9). The greatest risk factor for kidney stone formation is hypercalciuria (10). In most instances, the underlying mechanisms of hypercalciuria are not clinically evident (i.e., no systemic cause identifiable) and hence the term idiopathic hypercalciuria is employed (11). The common definition of idiopathic hypercalciuria is urinary excretion of calcium higher than the eightieth percentile for healthy individuals (i.e., >250 mg/day in women and 300 mg/day in men). Idiopathic hypercalciuria is a heritable trait but strongly influenced by dietary factors. Increased intestinal calcium absorption, augmented bone resorption, and renal calcium leak can cause an excess of calcium excretion in urine in idiopathic hypercalciuria (12). Despite increased intestinal calcium absorption, urinary calcium losses exceed dietary calcium absorbed, and therefore individuals with idiopathic hypercalciuria are often in negative calcium balance. Idiopathic hypercalciuria therefore not only increases the risk for calcium-containing kidney stones but also is associated with reduced bone mineral density and increased fracture risk (13). As a consequence, treatments aimed at reducing urinary calcium excretion both reduce recurrence risk of stones and attenuate bone mass loss.

This review focuses on the molecular mechanisms that contribute to tubular calcium transport in kidney, intestine, and bone, with emphasis on areas implicated in hypercalciuria that lead to stone disease. Hyperoxaluria is also a significant risk factor for calcium-oxalate kidney stone formation; however, we have elected to not discuss the causes of hyperoxaluria and instead refer the reader to recent reviews (14, 15). The precipitation of calcium-oxalate or calcium-phosphate is inhibited by urinary citrate, with low urinary citrate excretion being a risk for calcium kidney stones. Citrate metabolism and its contribution to stone disease are reviewed in detail elsewhere (16).

MECHANISMS OF INTRARENAL CALCIUM PRECIPITATION

Under certain circumstances, calcium-oxalate and calcium-phosphate leave the soluble phase in urine and form solid deposits in the kidney (crystallization), in the form of either tissue deposits (nephrocalcinosis) or as kidney stones outside of/attached to parenchymatous structures (nephrolithiasis). The primary physicochemical processes leading to nephrocalcinosis and nephrolithiasis are similar and governed by the principle of supersaturation. If a calcium salt in the urine exceeds the solubility limit (which can be determined empirically), the solution is supersaturated. The level of supersaturation can be expressed as the ratio of the concentration of the dissolved salt to its solubility (17). If solid seeds are added to a supersaturated solution, crystallization occurs on the surface of the seeds and depletes the solution back to solubility. Without solid seeds, the solution remains clear, with supersaturation increasing with the continued addition of salt (either calcium-oxalate or calcium-phosphate) until a critical empirical limit is reached, and spontaneous nucleation occurs. This critical upper limit is known as the upper limit of metastability (ULM). Both supersaturation and ULM for calcium-oxalate and calcium-phosphate can be determined in human urine (18). The ULM strongly correlates with the corresponding supersaturation in the urine, a phenomenon that remains poorly understood

(17). In human urine, the ULM is considerably above supersaturation (2- to 11-fold above supersaturation for calcium-phosphate and 11- to 50-fold for calcium-oxalate), reflecting the presence of urinary factors that prevent crystallization (i.e., citrate, pyrophosphate, phytate, and proteins). Empirical ULM determinations of urine are cumbersome and no robust commercial assays are available. Because ULM is tightly linked to supersaturation and the latter can easily be determined, urinary supersaturation is typically used clinically to guide therapy. Urinary supersaturations determined on ambulatory 24-h urine collections accurately reflect the long-term average urinary supersaturation, and thus crystallization forces, and strongly correlate with kidney stone composition. Moreover, therapies that reduce stone recurrence strongly correlate with reductions in urinary supersaturation (18–21). Despite multiple lines of defense, urinary crystal formation occurs in most humans. In calcium stone formers, urinary crystal formation exceeds physiological limits, resulting in the formation of large aggregates of calcium-oxalate or calcium-phosphate in complex with urinary proteins, also known as kidney stones.

Although calcium-oxalate and calcium-phosphate supersaturation are key drivers of stone formation in people with calcium stones, the early pathogenetic events leading to kidney stone formation greatly differ, depending on stone type, comorbid conditions, and urine chemistry. Three different pathways leading to kidney stone formation have been recognized thus far: (*a*) stones attached to the kidney papilla at sites of interstitial calcium-phosphate plaques (known as Randall plaques) as typically seen in idiopathic calcium-oxalate stone formers, (*b*) stones attached to plugs obstructing terminal ducts of Bellini as typically seen in calcium-phosphate stone formers or in persons with secondary forms of calcium-oxalate stones, and (*c*) stones forming in free solution in the renal collecting system (e.g., medullary sponge kidney) (22). In this review, we focus on the two most common pathways, plaque- and plug-dependent calcium stone formation. In both pathways, kidney stone formation starts with calcium-phosphate (apatite) crystallization, either in the interstitium (Randall plaque) or in the intratubular compartment (plug). Both processes were first described by Alexander Randall (23). Research over the past 25 years has shed additional light on the underlying processes.

The earliest lesions in Randall plaque formation are multilayered spherulites composed of apatite and matrix in basement membranes of thin loops of Henle, followed by interstitial spherulite formation on type 1 collagen fibers in the adjacent interstitial space (24). Spherulite fusion then leads to the formation of large interstitial plaque beneath the urothelium. Upon breaching the urothelium, urinary proteins (Tamm-Horsfall and osteopontin) and amorphous apatite overlay the plaque. As plaque overgrowth increases, conversion of apatite to calcium-oxalate occurs, ultimately leading to a cauliflower-like calcium-oxalate outgrowth visible macroscopically as a kidney stone. This sequence of events appears to be the primary mechanism of kidney stone formation in idiopathic calcium-oxalate stone formers, which are by far the most common. The vas washdown hypothesis has been used to explain Randall plaque formation (25). Individuals with idiopathic hypercalciuria display reduced proximal tubular sodium and consequently calcium reabsorption, which results in increased distal tubular calcium delivery that leads to compensatory increased calcium reabsorption from the thick ascending limb of Henle's loop (TAL) (26). Calcium reabsorbed from the TAL (without water) enters the descending vasa recta (located inside a ring of surrounding medullary thick ascending limbs). Due to the countercurrent mechanism, the calcium concentration is expected to increase in the inner medulla, thereby promoting apatite crystallization on collagen fibers of basement membranes of thin loops.

Kidney stone formation on intraluminal deposits (tubular plugs) is the second mechanism mediating nephrolithiasis, typically observed in calcium stone formers with primary or enteric hyperoxaluria (calcium-oxalate) or calcium-phosphate stones (apatite or brushite). Plugs are located primarily in the inner medullary collecting ducts (IMCDs) or ducts of Bellini and are associated

with destruction of adjacent tubular cells and surrounding interstitial fibrosis. Plugs protrude at openings of ducts of Bellini in the urinary space and can function as sites of local overgrowth of kidney stone formation, which is driven by the prevailing supersaturation of calcium-oxalate or calcium-phosphate. Stone formation on tubular plugs has been observed in all types of stone formers except for calcium-oxalate stone formers with idiopathic hypercalciuria (22). In stone formers with primary hyperparathyroidism, primary hyperoxaluria, and brushite stones, plugs may extend more proximal beyond the IMCD and have even been observed in proximal tubules of stone formers with primary hyperoxaluria. Hence, elevated urinary calcium plays a primary role in plaque and plug formation, the two major pathways of kidney stone formation. The basic mechanisms driving these processes still remain poorly understood and warrant further study.

ALTERED RENAL TUBULAR CALCIUM HANDLING

Ionized calcium is freely filtered at the glomerulus, with most (>98%) reabsorbed along the course of the nephron. Most of this calcium (>60%) is reabsorbed from the proximal tubule predominantly by a paracellular pathway. The TAL reabsorbs a significant amount of the filtered calcium (20–25%) via a regulated paracellular pathway. The remainder of calcium reabsorption (5–10%) occurs via a tightly regulated transcellular mechanism from the distal convoluted tubule (DCT) and connecting tubule (CNT). Over the past 20 years our understanding of the molecular components involved in these processes, with abnormalities in these transport processes being implicated in the development of hypercalciuria and kidney stone formation, has increased significantly. Consideration of urinary calcium excretion would not be complete without discussion of intestinal calcium absorption, as well as formation of and resorption from bone. Newer insights into these molecular mechanisms are provided to highlight their role in regulating urinary calcium excretion and how they contribute to the risk for calcium kidney stone formation.

The Proximal Tubule

Most filtered calcium is reabsorbed from the proximal tubule (>60%), with most reabsorption (90%) occurring through a passive paracellular process (27, 28). Therefore, it is not surprising that defects in calcium reabsorption from the proximal tubule have been implicated in the pathogenesis of hypercalciuria in calcium kidney stone formers (29, 30), highlighting the importance of understanding the molecular mechanism that mediates calcium reabsorption from the proximal tubule. The driving force for calcium reabsorption from the proximal tubule is the movement of sodium, which creates an osmotic gradient for the reabsorption of water (27) (**Figure 1**). The removal of water from the lumen of the proximal tubule increases the calcium concentration, thereby generating a concentration gradient, down which calcium can flow via the paracellular shunt. As such, the proximal tubule epithelium is leaky with a very low transepithelial resistance (measuring 5–15 $\Omega^* \text{ cm}^2$) (31, 32). The ultrafiltrate–to–tubular fluid (UF/TF) ratio for calcium is reported to be nearly equivalent (1.0–1.2) (27, 33, 34), and the flux of calcium is nearly always equivalent to sodium, consistent with its passive paracellular reabsorption (33). These observations suggest that convective flux of water across the proximal tubule may drive paracellular calcium reabsorption via a process called solvent drag (28). Recent mathematical modeling data, however, argue against a significant fraction of calcium being reabsorbed by a convective process, but definitive experimental studies have not been completed (35).

The apical influx of sodium into the proximal tubule occurs primarily in exchange for a proton, a process mediated primarily by the epithelial sodium proton exchanger NHE3 (encoded by *SLC9A3*), with efflux predominantly occurring through the sodium-potassium-ATPase (Na^+K^+ATPase) (36). *Slc9a3* null animals demonstrate increased urinary calcium excretion

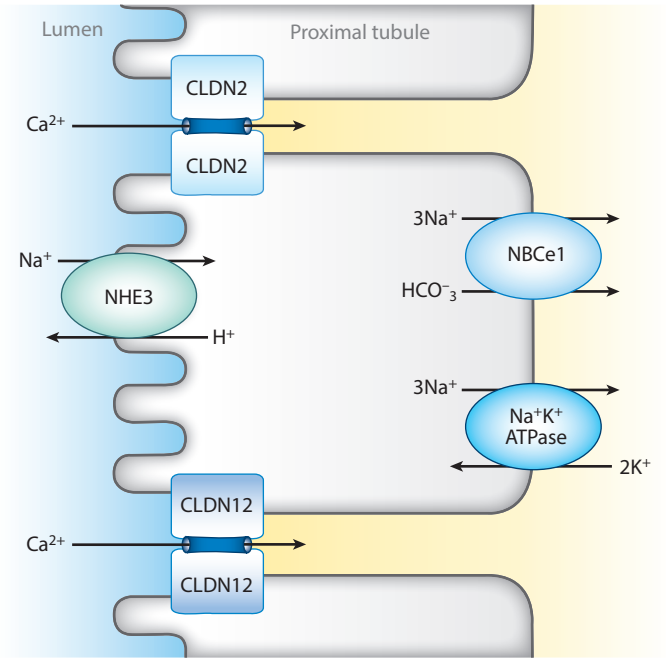

Figure 1

Molecular pathway of calcium transport in the proximal tubule. Sodium reabsorption is mediated primarily by apical influx via the epithelial sodium proton exchanger NHE3 and basolateral secretion by the sodium-potassium-ATPase (Na^+K^+ATPase) and the electrogenic sodium bicarbonate cotransporter (NBCe1). This drives paracellular calcium reabsorption through claudin-2 (CLDN2) or claudin-12 (CLDN12) pores.

(but not renal calcifications) (37). However, children with deleterious *SLC9A3* mutations have congenital sodium-losing diarrhea, as NHE3 is also present in the intestine, where it contributes significantly to sodium and likely also calcium reabsorption (38, 39). However, urinary calcium excretion has not been examined in these patients. The remainder of sodium reabsorption from the proximal tubule is contributed by a myriad of apical transporters, including NHE8/*SLC9A8*, and the sodium–glucose cotransporters SGLT1 and SGLT2. The role of NHE8 in paracellular calcium reabsorption from the proximal tubule is not known, although NHE8 function appears to regulate the small amount of transcellular calcium reabsorption that occurs in the distal part of this segment (27, 40). SGLT2 inhibition in healthy volunteers led to a slight increase in urinary calcium and sodium excretion, supporting the claim that SGLT-driven sodium reabsorption drives water and consequently calcium reabsorption from the proximal tubule (41). Consistent with this finding, hypercalciuria has also been observed in patients with familial renal glucosuria (42).

Water reabsorption across the proximal tubule occurs predominantly (~70%) via a transcellular pathway, with the remainder moving through the leaky paracellular tight junction (43). Transcellular water reabsorption occurs through the water channel aquaporin-1 (AQP1), which is expressed in both the apical and the basolateral membranes in this segment (43, 44). The coupling of water flux to calcium reabsorption across the proximal tubule is consistent with single nucleotide polymorphisms (SNPs) in *AQP1* associating with kidney stone formation (45). Exactly how these SNPs contribute to increased risk for kidney stone formation is not known, although it could be speculated that reduced AQP1 water permeability may increase water flux through the

paracellular pathway, thereby increasing calcium reabsorption and thus reducing risk for kidney stone formation.

Calcium is a divalent cation, with a valence of +2. Thus, the electrical potential difference across the proximal tubule could significantly affect the driving force for paracellular calcium reabsorption. Reabsorption of ions and small molecules along the length of the proximal tubule is not uniform. In the first part of the proximal tubule there is significant SGLT2-mediated absorption of glucose, which is electrogenic because it is coupled to sodium, yielding an approximately −2 mV potential difference (46). Bicarbonate is also absorbed preferentially in the first part of the proximal tubule, contributing to an increased concentration of chloride. This increase provides the driving force for paracellular chloride reabsorption, which by the late S2 proximal tubule segment results in a net lumen-positive potential difference (~+2 mV) (27). This in turn creates a favorable electrochemical gradient for paracellular calcium reabsorption from the late proximal tubule.

In order for paracellular reabsorption to occur, there must be not only a driving force but also permeability of the epithelia (35). The proximal tubule is highly permeable to calcium (27). However, our understanding of how paracellular permeability is conferred to the proximal tubule has significantly increased in the past few years. Claudins are four-pass membrane proteins, with the C and N termini in the cytosol, that localize to the tight junction (47). Interaction with claudins in the same cell (*cis*) or adjacent cell (*trans*) confers permeability to the tight junction (47). Claudin-2 (CLDN2), CLDN10a, CLDN12, and likely CLDN17 are expressed in the proximal tubule (48). CLDN10a and CLDN17 are anion-selective claudins and likely contribute chloride permeability to this segment. In contrast, CLDN2 and CLDN12 are cation-selective claudins recently implicated in contributing the calcium permeability of this segment (32, 49). Proximal tubules from *Cldn12* knockout mice display reduced sodium and calcium permeability when perfused ex vivo and permeability assessed by bionic diffusion potential measurements (32). However, these animals do not display hypercalciuria, suggesting altered expression or function of CLDN12 does not contribute to hypercalciuria in humans (32). In contrast, direct measurements of the calcium permeability of proximal tubules from *Cldn2* knockout mice have not been reported. However, *Cldn2* knockout mice display increased urinary calcium excretion relative to wild-type littermates, even on a low-calcium diet, consistent with a primary renal calcium leak (49). Failed calcium reabsorption from the proximal tubule is likely the cause of the increased urinary calcium excretion, as CLDN2 is expressed only in the proximal tubule and thin descending limb and the expression of other mediators of calcium reabsorption is not altered (49, 50). Finally, genetic variations in *CLDN2* associate with kidney stones and a likely deleterious mutation in *CLDN2* causes hypercalciuria and kidney stones (49).

The proximal tubule is where 25-hydroxyvitamin D is converted to 1,25-dihydroxyvitamin D, the active form of vitamin D, and is inactivated by 24-hydroxylation. The enzyme responsible for the latter enzyme reaction is 1,25-dihydroxyvitamin D_3 24-hydroxylase (CYP24A1). Mutations in this gene result in elevated levels of 1,25-dihydroxyvitamin D in plasma, hypercalcemia, hypercalciuria, and nephrolithiasis in infants, a condition called idiopathic infantile hypercalcemia (51). Mutations in the proximal tubule sodium-phosphate cotransporters *SLC34A1* and *SLC34A3* also result in conditions with hypercalciuria, although this is a secondary effect. Mutations in *SLC34A1* cause a syndrome similar to that caused by mutations in *CYP24A1* (idiopathic infantile hypercalcemia); however, these patients display urinary phosphate wasting and hypophosphatemia as well as hypercalciuria and hypercalcemia (52). Patients with mutations in *SLC34A3* tend to display symptoms later as children and present with hereditary hypophosphatemic rickets with hypercalciuria (53). Both disorders of primary renal phosphate wasting display hypercalciuria due to increased levels of 1,25-dihydroxyvitamin D in plasma, which increase calcium absorption from the gut and resorption from bone.

Two diuretics primarily target the proximal tubule: osmotic diuretics such as mannitol and carbonic anhydrase inhibitors such as acetazolamide. Osmotic diuretics work by retaining water in the tubular lumen, thereby preventing reabsorption. Because most water is reabsorbed from the proximal tubule, the action of osmotic diuretics is largely ascribed to this segment. Due to close coupling of water and calcium reabsorption from the proximal tubule, it is not surprising that higher doses of mannitol (i.e., 10–20%) increase urinary calcium excretion because of reduced reabsorption from the proximal tubule (54). However, lower doses of mannitol do not confer this effect, likely due to compensation by downstream nephron segments (54). Acetazolamide, a common carbonic anhydrase inhibitor, causes increased urinary calcium excretion and reduced calcium reabsorption from the proximal tubule (54). The calciuria is likely a consequence of the inhibition of carbonic anhydrases in the proximal tubule, which are required to catalyze the conversion of H_2O and CO_2 into protons and bicarbonate, a step prerequisite for NHE3 activity and thus sodium reabsorption. Regardless, the hypercalciuric effect of carbonic anhydrase inhibitors combined with hypocitraturia, which they also cause, increases risk for kidney stone formation (55).

The Thick Ascending Limb of the Loop of Henle

Transport of calcium across the TAL is critical for the maintenance of overall calcium homeostasis. Consequently, failure of TAL transport severely diminishes the renal reabsorptive capacity for this cation. As much as 25% of calcium filtered by the kidney is reclaimed along the length of the TAL via a paracellular pathway made up of pore-forming claudins (56). The TAL generates a lumen-positive transepithelial voltage that provides a critical driving force for reabsorption of calcium via the paracellular shunt (57).

This transepithelial potential difference is generated by the asymmetrical secretion of electrolytes across the TAL (**Figure 2**). In brief, the furosemide-sensitive cotransporter NKCC2 (encoded by *SLC12A1*) is highly and specifically expressed along the length of the TAL and is the main uptake mechanism for sodium, potassium, and chloride in this segment. NKCC2 cotransports sodium, potassium, and two chloride ions across the apical membrane (58–60). The inwardly cotransported sodium is secreted basolaterally by the Na^+K^+ATPase, which provides the main driving force for sodium reabsorption across this segment. The chloride ions leave the cell via CLCNKB channels situated in the basolateral membrane. Chloride exit is driven by the transmembrane potential difference, which is negative intracellular and maintained around −80 mV (59). Potassium is recycled back across the apical membrane via renal outer medullary potassium (ROMK; *KCNJ1*) channels (59, 61). Because the diffusion potential for potassium across the apical membrane is higher than the diffusion potential of chloride across the basolateral membrane, a lumen-positive transepithelial voltage is generated.

This lumen-positive transepithelial potential difference increases from approximately +5–13 in the inner stripe of outer medulla ($mTAL_{ISOM}$) to approximately +30 mV in the cortical TAL (60). This larger diffusion potential across the cortical TAL is best detected in microperfusion experiments with low perfusion rates and is likely the result of interstitial sodium backflux into the tubular lumen via the paracellular shunt rather than by active transport mechanisms (60). The voltage gradient can be inhibited by furosemide, a NKCC2 inhibitor (54). Reduction in the lumen-positive transepithelial voltage by furosemide collapses the transepithelial potential difference, resulting in marked inhibition of TAL calcium transport and urinary calcium wasting (54). Consistent with this finding, loop diuretics, such as furosemide, cause hypercalciuria (54), and premature babies receiving furosemide often develop nephrocalcinosis, which in 50% of cases resolves 6 months after discontinuation (62).

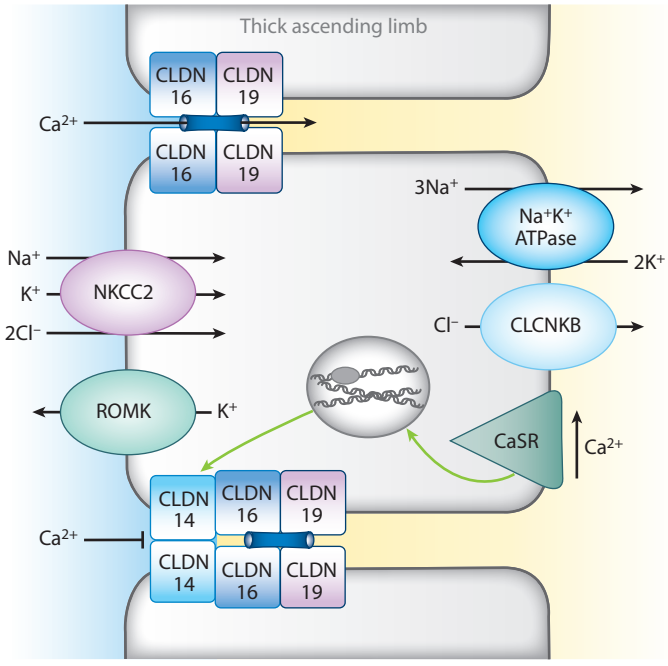

Figure 2

Molecular pathway of calcium transport in the thick ascending limb of the loop of Henle. The combined transport of sodium, potassium, and two chloride ions through the sodium-potassium-chloride cotransporter (NKCC2) is coupled to basolateral efflux of sodium through the sodium-potassium-ATPase (Na^+K^+ATPase) and chloride through the CLCNKB channel as well as luminal recycling of potassium through the renal outer medullary potassium (ROMK) channel. This contributes to a lumen-positive potential, which favors paracellular calcium reabsorption through a tight junction pore composed of claudin-16 (CLDN16) and claudin-19 (CLDN19). Increased blood calcium activates the calcium-sensing receptor (CaSR), leading to increased transcription of the cation-blocking claudin-14 (CLDN14).

Mutations in genes encoding this TAL transport pathway lead to Bartter syndrome (58, 61, 63), a disease characterized by marked renal NaCl wasting, hyperreninemia, hypokalemia, metabolic alkalosis, and hypotension (60). Importantly, mutations in *SLC12A1* and *KCNJ1* cause a severe form of Bartter syndrome, termed antenatal Bartter syndrome, which presents with polyhydramnios and is often associated with premature birth. In these forms of Bartter syndrome, patients experience severe calcium wasting, which leads to early-onset nephrocalcinosis (64). In fact, a severe form of antenatal Bartter's syndrome that resolves spontaneously as an infant ages was recently identified. The syndrome is due to mutations in *MAGED2*, a gene important for regulating the expression of cotransporters, including NKCC2 (65). Importantly, these patients suffer from hypercalciuria, which resolves with the renal salt wasting, although nephrocalcinosis persists in several patients (65). In the classical form of Bartter syndrome due to mutations in *CLCNKB*, there is larger phenotypic variability, including less-severe cases. Hypercalciuria and the related sequelae are not frequently observed in these patients (63). The reason for this remains to be fully delineated, as all mutations are predicted to impair the generation of the lumen-positive voltage gradient across the TAL, although the effect of *CLCNKB* mutations may impair the electric potential across the TAL less than that found in the antenatal forms.

Calcium transport predominates in the cortical portion of the TAL, with paracellular calcium transport across the $mTAL_{ISOM}$ being markedly lower (66). This decrease is contributed in part by the permeability characteristics of the TAL, which are complex and vary between the $mTAL_{ISOM}$, the outer stripe of outer medulla ($mTAL_{OSOM}$), and the cortical TAL. The paracellular shunt of the TAL is cation selective, with sodium permeability (P_{Na}) 2–10 times higher than chloride permeability (P_{Cl}) along the entire segment (67). The permeability to divalent cations increases along the length of the TAL and is the lowest in the $mTAL_{ISOM}$ (67). Conversely, sodium permeability is highest in the $mTAL_{ISOM}$, where nearly half of the sodium reabsorption occurs via a paracellular pathway (67). The permeability characteristics of this segment are dependent on the expression profile of specific claudins. Three claudins are predominantly expressed along the length of the TAL and have been linked to the permeability characteristics of the epithelium: CLDN10, CLDN16, and CLDN19. CLDN16 and CLDN19 likely contribute calcium- and magnesium-permeable pores to the TAL, and CLDN10 allows the permeation of sodium across the epithelium.

Mutations in *CLDN16* and *CLDN19* were identified as causative in the rare genetic disease familial hypomagnesemia with hypercalciuria and nephrocalcinosis (FHHNC) (68, 69). Patients affected with the disorder have marked perturbations of their mineral balance, including severe hypomagnesemia as a consequence of severe renal calcium and magnesium wasting (68, 69). This type of renal wasting leads to nephrocalcinosis, which often results in renal insufficiency. Loss of renal expression of these claudins is responsible for the clinical phenotype, as the urinary losses of calcium and magnesium were reversed in a patient with FHHNC after a renal transplant (70). *Cldn16*-deficient mice replicate the renal phenotype with marked renal calcium and magnesium wasting and hypomagnesemia (71). Tubular microperfusion of TAL segments from these animals revealed markedly decreased P_{Ca} and magnesium permeability (P_{Mg}) compared with P_{Na}, while the P_{Na}/P_{Cl} ratio was unaltered. Furthermore, CLDN16 and CLDN19 directly interact to confer cation selectivity in cell model systems, which explains why mutations in one gene are sufficient to cause the disease (72).

Expression of CLDN16 and CLDN19 has been localized to basolateral membrane domains and to the tight junction of TAL cells in kidney (67). While the function of CLDN16 and CLDN19 in basolateral domains is unknown, the tight junction localization likely confers the specific permeability characteristics of this epithelium. Tight junction expression of CLDN16 and CLDN19 occurs in the $mTAL_{OSOM}$ but more so in the cortical TAL, and CLDN10 is the predominant claudin in the $mTAL_{ISOM}$, although it is also expressed in more cortical segments (67). There is a mosaic expression of claudins in the $mTAL_{OSOM}$ and cortical TAL, with CLDN16 and CLDN19 localizing to specific cell-cell contacts and CLDN10 localizing to other contacts (67). Thus, CLDN16 and CLDN19 are present in tight junctions different from those in which CLDN10 is present in the TAL. Consistent with the molecular heterogeneity of this segment, there is substantial evidence for cellular diversity in transport capabilities and morphology as well (60). In human kidney, recent observations have mapped two types of TAL cells via single-cell RNA sequencing. Here, the expression of *CLDN16* predominates in one cell type, and the other cell type has a high expression of *CLDN10* (73). Recent similar findings have been demonstrated in mouse kidney (74). Elegant experiments conducted by Milatz et al. (67) demonstrated the requirement of CLDN16 and CLDN19 to confer divalent cation permeability by coupling perfusion of single mouse $mTAL_{ISOM}$, $mTAL_{OSOM}$, and cortical TAL tubules with claudin expression profiling by immunohistochemistry of individual tubules. The authors measured P_{Mg} as an assessment of divalent cation permeability and found that the P_{Mg}/P_{Na} ratio was more than threefold higher in the cortical TAL, where CLDN16 predominated, than in the $mTAL_{ISOM}$ (67). Overall, these observations are consistent with CLDN16 and CLDN19 complexes forming pores permeable to

calcium and magnesium and CLDN10 forming pores permeable to sodium. Furthermore, these findings explain the different permeability characteristics and to some extent the different reabsorptive properties along the length of the TAL.

The specific deletion of *Cldn10* from the distal nephron, including the TAL in mice, using the *Ksp*-Cre alters paracellular permeability in the TAL not only to sodium but also to divalent cations (75). Microperfusion of these tubular segments revealed loss of P_{Na} over P_{Cl} as would be predicted if CLDN10 confers sodium permeability. This in turn markedly increased the lumen-positive voltage. Importantly, deletion of *Cldn10* from the TAL also increased P_{Ca} and P_{Mg} compared with P_{Na}, which coincides with a redistribution of CLDN16 to the $mTAL_{ISOM}$ (76). Furthermore, potentiation of the lumen-positive transepithelial potential (75, 76) may serve to augment renal reabsorption of calcium and magnesium in these animals. In fact, deletion of *Cldn10* from the distal nephron results in increased renal reabsorption of both calcium and magnesium and promotes the development of nephrocalcinosis, consistent with nephrocalcinosis caused by increased TAL calcium reabsorption (75).

Calcium transport in the TAL is regulated by several calciotropic hormones (66, 77). Parathyroid hormone (PTH) increases calcium and magnesium reabsorption from this segment by affecting both the transepithelial voltage and the permeability of the paracellular shunt (77). The mechanism by which this latter process occurs remains to be determined in detail. However, in cell models, a protein kinase A (PKA) phosphorylation site on Ser217 in CLDN16 is required for its localization to the tight junction, suggesting that increased PKA activity mediated by PTH may play a role (78). Another key regulator of calcium transport in the TAL is the calcium-sensing receptor (CaSR), which is expressed along the basolateral membrane of this segment. Here, the CaSR senses changes in serum calcium concentration and adjusts tubular reabsorption accordingly. Increases in extracellular calcium increase intracellular calcium levels and the production of inositol trisphosphate and markedly reduce vasopressin-dependent cyclic AMP accumulation (79). Acute changes in calcium transport in response to alterations in extracellular calcium have also been observed in isolated and perfused cortical TALs. Acute activation of the CaSR by increased bath calcium markedly inhibits net flux in the TAL. Importantly, these changes occur without changes in the membrane voltage across the epithelium and without changes in sodium and chloride fluxes (79). Calcimimetics are drugs that enhance CaSR sensitivity to calcium, whereas calcilytics block CaSR function. These drugs have been used to study CaSR function in various epithelia. Acute application of calcilytics to perfused cortical TALs increases net calcium flux and calcium permeability, again without changes in sodium and chloride fluxes or the transepithelial voltage. These findings are in line with CaSR activation directly attenuating calcium permeation of the paracellular shunt (80).

CaSR activation also potently stimulates expression of CLDN14 in the kidney (81–85). *CLDN14* was originally found to be mutated in individuals with nonsyndromic deafness, as CLDN14 is also expressed in the organ of Corti; however, these individuals do not have alterations in renal calcium handling (86). A role in renal calcium handling was implicated when a large genome-wide association study linked SNPs in *CLDN14* to hypercalciuria, kidney stones, and reduced bone mineral density. Renal CLDN14 expression was subsequently shown to increase when serum calcium increases, via activation of the CaSR (81–84). Dietary calcium intake and administration of 1,25-dihydroxyvitamin D_3 also alter *Cldn14* messenger RNA and CLDN14 protein expression, indirectly by increasing serum calcium and thereby activating the CaSR (81–85). Chronic pharmacological activation of the CaSR with the calcimimetic cinacalcet leads to a pronounced 40-fold increase in *Cldn14* expression (81), and more rapid effects only 2 h after calcimimetic administration have also been described (82). CLDN14 expression is observed predominantly in the cortical TAL after a high-calcium diet (85). We have recently developed an antibody

against CLDN14 that works on structurally well-preserved paraffin-embedded sections. Using this antibody, we observed renal CLDN14 expression only in hypercalcemic animals (84). In mice made hypercalcemic through the use of a vitamin D analog, CLDN14 was restricted to a subset of cells in the $mTAL_{OSOM}$ and cortical TAL that also expressed CLDN16 but not CLDN10 (84).

Overexpression of *CLDN14* in cell lines alters the permeability characteristics of the paracellular shunt. Specifically, *CLDN14* overexpression reduces the permeability to calcium and the P_{Na}/P_{Cl} ratio, consistent with a pore-blocking effect (81, 83, 87). CLDN14 interacts specifically with CLDN16 but not directly with CLDN19 (83). Cortical TALs expressing CLDN14 after a high-calcium diet have reduced permeabilities to both calcium and magnesium (83). Based on the localization and changes in permeability characteristics, CLDN14 expression likely blocks divalent-cation-permeable pores formed by CLDN16 and CLDN19 (84). As such, the CaSR likely acts to prevent hypercalcemia via upregulation of CLDN14, thereby reducing paracellular calcium permeability in the TAL and increasing renal calcium excretion and ultimately lowering blood calcium levels. Evidence from genetic models of *Cldn14* deletion and overexpression is in line with these observations. *Cldn14* knockout mice placed on a high-calcium diet have a lower fractional excretion of calcium than wild-type mice do (83). Conversely, transgenic mice overexpressing CLDN14 in all TAL cells increased the fractional excretion of calcium. Furthermore, activating mutations in the CaSR leads to autosomal-dominant hypocalcemia, with associated hypercalciuria visible at presentation or following treatment to raise serum calcium levels (88). Finally, rare activating mutations in the CaSR are so severe that they markedly change overall TAL transport, resulting in a form of Bartter syndrome with hypocalcemia (88).

The Distal Convolution

The distal convolution is an anatomical structure that includes the DCT, the CNT, and the initial portion of the collecting duct (CD) (56). In these segments, filtered calcium is reclaimed via an active transcellular pathway. Micropuncture studies estimate 3–7% of filtered calcium is reabsorbed along the length of the distal convolution (54). The DCT segment can be identified by the expression of the thiazide-sensitive NaCl cotransporter (NCC; encoded by *SLC12A3*) (89) and subdivided into the segments DCT1 and DCT2, where the DCT2 segment also coexpresses the epithelial sodium channel (ENaC). Little paracellular transport is thought to occur in the distal convolution, consistent with this epithelium having a high transepithelial resistance that increases along its length (56).

Calcium moves unidirectionally across the distal convolution via an active transcellular route (90) (**Figure 3**). The key transport proteins involved in this process have been identified. Transient receptor potential vanilloid 5 (TRPV5) is the main entry pathway for calcium in the apical membrane (54, 91). The channel was originally identified from rabbit primary cultures generated from tubules isolated from the CNT and CD (91), and the channel subsequently localized to rabbit CNT (54). However, expression of Trpv5 in mice extends to the DCT2 segment as well as the initial portion of the CD (54), but its distribution in humans has not been determined. The calcium-binding protein calbindin-D_{28K} (Calb28K) is also abundantly expressed in these cells, where it acts as a calcium buffer that can transport calcium from the apical entry site to the basolateral membrane without perturbing cellular calcium signaling (92). The proteins Na^{2+}/Ca^{2+} exchanger type 1 (NCX1) and plasma membrane Ca^{2+}-ATPase 4 (PMCA4) (93, 94) are the primary mechanisms mediating calcium extrusion across the basolateral membrane.

The role of TRPV5 in calcium reabsorption from the distal convolution is largely based on findings from mice with a targeted deletion of *Trpv5*. These animals show marked disturbances in calcium homeostasis, with severe hypercalciuria, decreased bone mineral density, and vitamin

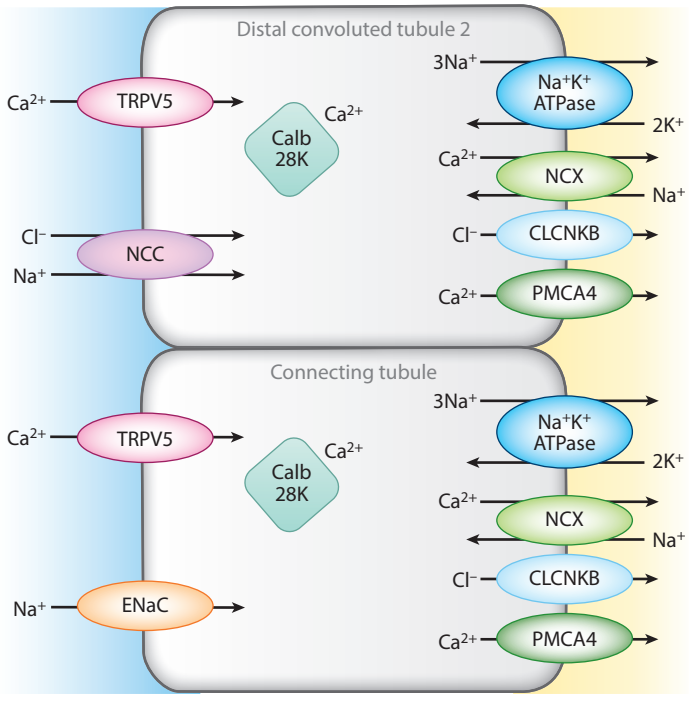

Figure 3

Molecular pathway of calcium transport from the distal convolution. Apical calcium entry occurs through the transient receptor potential vanilloid 5 (TRPV5) channel expressed primarily in the distal convoluted tubule 2 (DCT2) and connecting tubule (CT). Calcium binds to the buffering protein calbindin-D_{28K} (Calb28K), which shuttles calcium to the basolateral membrane, where export is mediated by Na^{2+}/Ca^{2+} exchanger (NCX) or plasma membrane calcium-dependent ATPase 4 (PMCA4). The distal convoluted tubule 1 expresses the NaCl cotransporter (NCC), DCT2 expresses both NCC and the epithelial sodium channel (ENaC), and CT cells express only ENaC. All of these segments express the CLCNKB chloride channel.

D–dependent intestinal calcium hyperabsorption (95). The hypercalciuria is driven by impaired calcium reabsorption from the distal convolution, as evidenced by micropuncture of the superficial distal aspect of the segment. This finding revealed fractional calcium delivery to be substantially elevated in *Trpv5*-deficient mice, in line with a primary defect in calcium transport along the length of this segment (95). In humans, recurrent kidney stones have also been linked to rare variants in the *TRPV5* gene (96).

TRPV5 is regulated by many calciotropic hormones and other molecular factors. Transcription of TRPV5 is regulated in a 1,25-dihydroxyvitamin D_3–dependent manner (97). PTH increases channel abundance by increasing *Trpv5* transcription (98). Furthermore, PTH nearly doubles calcium reclamation between early and late collection sites along the distal convolution of the same nephron (99). PTH also increases channel activity independent of changes in expression via PKA-dependent phosphorylation, which increases channel open probability and calcium influx (100). Moreover, PTH activates protein kinase C, which inhibits TRPV5 endocytosis via a caveolae-dependent pathway (101). Several other factors affect TRPV5 function, including alterations in dietary calcium, regulation by sex hormones, and disturbances in acid–base balance (102, 103). Klotho is a protein expressed in the distal convolution and cleavage products are also found in the circulation. *Klotho*-deficient mice have hypercalciuria and nephrocalcinosis (104).

Klotho was initially identified as an enzyme that acts by hydrolyzing *N*-glycan-linked oligosaccharides, thereby increasing TRPV5 channel abundance at the plasma membrane (105). However, subsequent studies found Klotho acts as a nonenzymatic scaffold required for FGF23 signaling (106). Consistent with this finding, *Fgf23*-deficient mice and *klotho*-deficient mice have a similar phenotype with respect to altered membrane expression of TRPV5 and hypercalciuria (107).

Thiazides and thiazide-like diuretics block NCC in the DCT. Thiazides are most often prescribed to treat arterial hypertension but, in addition to their blood-pressure-lowering diuretic effect, significantly affect renal calcium handling. Thiazide treatment results in hypocalciuria, a property used to treat hypercalciuria in calcium kidney stone formers (108, 109). The effect of thiazides on renal calcium excretion is observed in patients with both hypo- and hyperparathyroidism, in line with them being PTH independent (109). Patients with mutations in the *SLC12A3* gene, and thus functional loss of the NCC cotransporter, develop Gitelman syndrome, which is characterized by renal NaCl wasting, hypokalemic metabolic alkalosis, hypocalciuria, and hypomagnesemia (110). The exact mechanisms mediating hypocalciuria following loss-of-function mutations in the *SLC12A3* gene or pharmacological treatment with thiazides are debated, but they are generally considered the result of changes in calcium transport in the proximal tubule, although an additional effect on the distal convolution has been described and reviewed in detail elsewhere (111). Volume contraction secondary to renal NaCl wasting in these conditions leads to compensatory increases in sodium reabsorption from the proximal tubule, which causes increased calcium reabsorption from the proximal tubule in addition to driving renal reclamation of NaCl. Micropuncture studies of *Slc12a3*-deficient mice support this conclusion (112). When NaCl restriction was imposed to reduce extracellular volume, a hypocalciuric effect was absent in *Slc12a3*-deficient mice (113). Furthermore, *Trpv5*-deficient mice display a potent hypocalciuric response to the administration of thiazides (114). Together, these studies highlight the central role that more proximal paracellular calcium reabsorption plays in response to the hypocalciuric effect of both thiazide administration and NaCl restriction.

INCREASED INTESTINAL CALCIUM ABSORPTION

Increased intestinal calcium absorption results in increased renal excretion when the capacity to deposit calcium in bone is exceeded, to prevent increased plasma calcium levels. Moreover, elevated plasma calcium not only increases urinary calcium excretion as described above but also directly feedback inhibits intestinal calcium absorption (81, 115). As outlined above, increased intestinal calcium absorption is a hallmark of stone formers with idiopathic hypercalciuria (116). Calcium is absorbed from the intestine via a saturable pathway present in the duodenum and proximal colon/cecum and an unsaturable pathway found throughout the small intestine and colon. These two observations are consistent with an active transcellular pathway (saturable) and a passive paracellular pathway (unsaturable) (34) (**Figure 4**).

Transcellular intestinal calcium absorption occurs via a mechanism analogous to the distal nephron. Apical calcium entry is mediated by TRPV6, buffering and shuttling to the basolateral membrane are mediated by calbindin-D_{9K}, and efflux is mediated by a calcium-dependent ATPase such as PMCA1b or NCX (117). Mice with genetic deletion of *Trpv6* and *EphB6* or engineered to express a nonfunctional Trpv6 demonstrate significant transcellular intestinal calcium absorption, even on a low-calcium diet, suggesting at least one other apical entry pathway (115, 118, 119). The apical voltage-gated calcium channel $Ca_v1.3$ has been proposed to contribute apical calcium influx from intestinal epithelium, although this has been contested (120, 121). An explanation for the conflicting results is that this pathway is present in younger but not older animals (122). Alternatively, intestinal deletion of transient receptor potential ion channel subfamily M, member 7

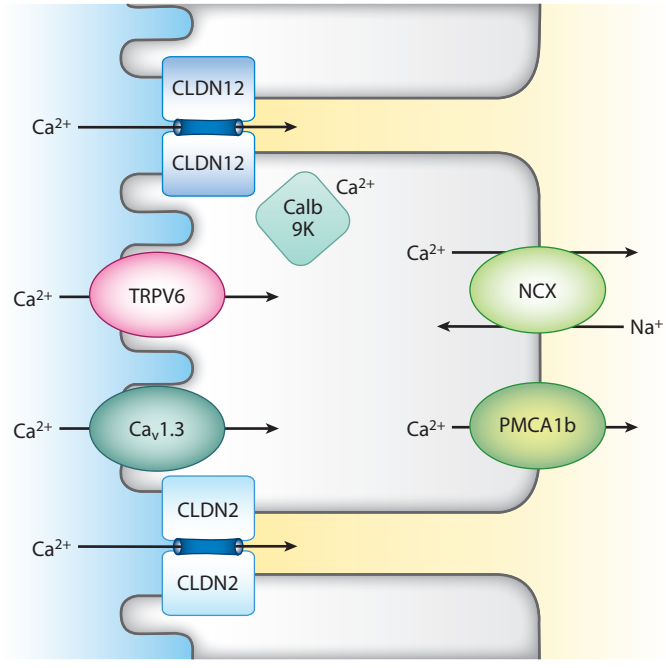

Figure 4

Molecular pathways of calcium absorption from the intestine. Transcellular calcium absorption from the duodenum and the colon is mediated via apical entry by transient receptor potential vanilloid 6 (TRPV6), buffering and shuttling are mediated by calbindin-D_{9K} (Calb9K), and basolateral efflux is mediated by Na^{2+}/Ca^{2+} exchanger (NCX) and plasma membrane calcium-dependent ATPase 1b (PMCA1b). Paracellular calcium absorption is proposed to occur through claudin-2 (CLDN2) and claudin-12 (CLDN12). The apical voltage-gated calcium channel $Ca_v1.3$ has also been proposed to mediate apical calcium influx.

(*Trpm7*) channel results in hypocalcemia, with appropriate hyperparathyroidism and increased 1,25-dihydroxyvitamin D, leading to the suggestion that TRPM7 can confer intestinal calcium absorption (123). The exact identity of the non-TRPV6 apical influx mechanism for transcellular intestinal calcium absorption is not clear; however, it is an area of active research.

1,25-Dihydroxyvitamin D, the primary hormone that stimulates intestinal calcium absorption, significantly upregulates the expression of Trpv6 in colon and duodenum (115, 124). This in turn increases intestinal calcium absorption via the transcellular pathway (n.b. 1,25-dihydroxyvitamin D also increases paracellular calcium absorption). Increased calcium influx into the epithelial cell increases calbindin-D_{9K} expression (125). Trpv6 transgenic overexpression in the intestine by the villin promoter results in increased intestinal calcium absorption and hypercalciuria (125). Moreover, individuals with a gain-of-function haplotype in *TRPV6* also display absorptive hypercalciuria and a propensity to kidney stone formation (126). These studies highlight how disorders giving rise to increased 1,25-dihydroxyvitamin D levels result in enhanced intestinal calcium absorption, enhanced renal excretion, and a tendency to form renal calculi.

Under conditions of normal calcium ingestion, most calcium absorption is proposed to occur via the paracellular route from the distal small intestine (34). As in the proximal tubule, paracellular calcium absorption occurs down its concentration gradient between cells. Cell culture work has implied a role for CLDN2 and CLDN12 in this process (127). Surprisingly, however, *Cldn12* knockout mice do not have altered intestinal calcium absorption and *Cldn2* knockout mice have

increased net intestinal calcium absorption, likely in response to a renal leak (32, 49). What is striking about the *Cldn2* knockout animal studies is that paracellular calcium permeability in the intestine was reduced only in the colon. This finding implies that decreased paracellular calcium secretion in the intestine across the colon of *Cldn2* knockout mice confers overall increased net absorption. Depending on the electrochemical gradient, paracellular calcium flux can lead to either secretion or absorption and the colon contributes net calcium absorption via both transcellular and paracellular pathways (128–130). Detailed evaluation of the *Cldn12* knockout mouse has not been reported. However, it is tempting to speculate that CLDN2 and CLDN12 confer redundant paracellular calcium permeability to the intestine, and only one claudin is required. More work is needed to clarify the identity of the paracellular calcium pore(s) in the intestine.

INCREASED BONE RESORPTION

Increased calcium release from bone is an important contributor to excessive calcium excretion in urine in idiopathic hypercalciuria. High levels of 1,25-dihydroxyvitamin D_3 in serum are common in idiopathic hypercalciuria and likely a mediator of both increased intestinal calcium absorption and increased calcium release from bone. In support of this, administration of 1,25-dihydroxyvitamin D_3 to normal subjects recapitulates these well-known features of idiopathic hypercalciuria, including the tendency to have a negative calcium balance on a low-calcium diet (131). Bone histomorphometry studies indicate reduced bone formation as the primary defect (13). Diet strongly influences urinary calcium excretion in stone formers with idiopathic hypercalciuria. As outlined above, sodium intake is a relevant and modifiable factor affecting calcium handling in the proximal tubule. A second important and modifiable factor of urinary calcium excretion is dietary acid intake (132). Overt metabolic acidosis is associated with increased urinary calcium excretion and an overall negative calcium balance (103). But even without systemic acidosis, there is a strong positive association between endogenous acid production and urinary calcium excretion (133). Both renal and extrarenal mechanisms are involved (103) (**Figure 5**). Hydroxylapatite [$Ca_5(OH/PO_4)_3$] in bone provides a gigantic buffer reservoir and is thus an important defense against the development of systemic acidosis. But this comes at a cost: Buffering of protons promotes loss of bone mass by both physicochemical mineral dissolution (acute) and cell-mediated bone resorption (chronic) via the activation of osteoclasts and the inhibition of osteoblasts (134). Large amounts of cations, mainly calcium, are released into the circulation during buffering and eliminated by the kidney (103). Glomerular filtration rate, plasma calcium, and hence filtered load of calcium remain constant during acid loading (135). Despite this, urinary calcium excretion increases in acidosis, reflecting altered tubular calcium handling. These changes are independent of PTH, 1,25-dihydroxyvitamin D_3, and tubular sodium handling (135, 136).

The bulk of calcium filtered at the glomerulus is reabsorbed from the proximal tubule and TAL by paracellular pathways. In the proximal tubule, sodium reabsorption by NHE3 drives paracellular calcium reabsorption. During chronic metabolic acidosis, NHE3 activity is increased and calcium reabsorption is increased, as expected (137). Micropuncture studies suggest calcium transport is unaltered in the TAL during chronic metabolic acidosis but inhibited in a segment after the early distal convoluted tubule puncture site (137). Follow-up experiments found the abundance and activity of the apical calcium entry channel TRPV5 in the DCT significantly reduced during metabolic acidosis (138, 139). In support of an important role of TRPV5 in acidosis-induced urinary calcium wasting, *Trpv5*-deficient mice were resistant to acidosis-induced urinary calcium increases, although these mice have markedly elevated urinary calcium excretion at baseline (139). Conflicting results exist for intestinal calcium absorption during metabolic acidosis: Increased, unaltered, and decreased calcium absorption have been observed (103). Hence, the contribution

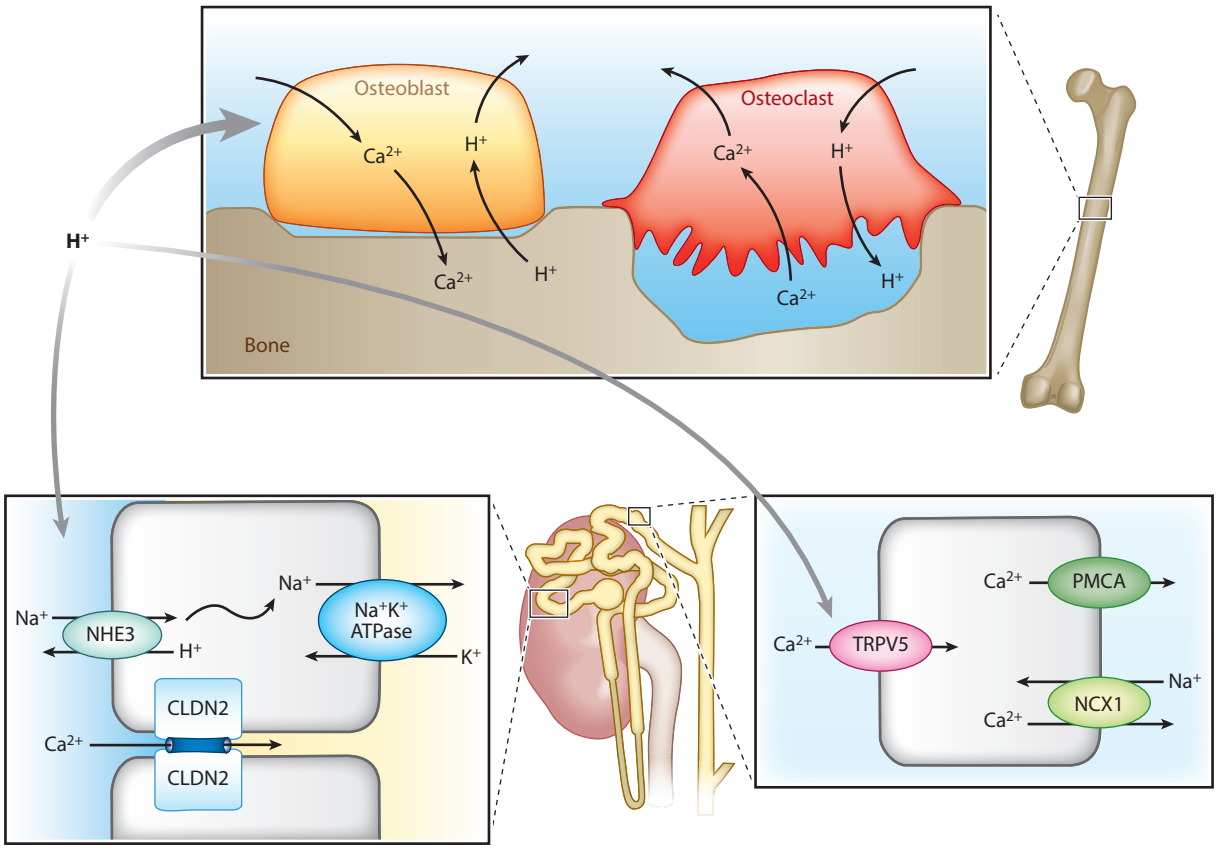

Figure 5

Effect of pH on calcium homeostasis. Acidosis stimulates calcium reabsorption from the proximal tubule by enhancing the expression of the epithelial sodium proton exchanger NHE3 and potentially inhibits reabsorption via attenuating transient receptor potential vanilloid 5 (TRPV5) activity. Regardless, there is physiochemical release of calcium from bone induced by acidosis, activation of osteoclasts, and inhibition of osteoblast activity, thereby favoring mineral release from bone. Note that paracellular Ca^{2+} reabsorption from the proximal tubule is driven by NHE3 and occurs through the paracellular Ca^{2+} pore composed of claudin-2 (CLDN2). Basolateral efflux of Ca^{2+} occurs in the distal convolution by a Na^{2+}/Ca^{2+} exchanger type 1 (NCX1) and a plasma membrane calcium-dependent ATPase (PMCA).

of intestinal calcium transport to overall calcium balance during metabolic acidosis remains unclear.

Large dietary acid loads (i.e., a Western diet rich in animal protein and poor in fruits and vegetables) or an inability to excrete endogenously produced nonvolatile acid equivalents as with distal tubular acidosis (dRTA) promotes formation of calcium-containing kidney stones through two key factors: an increase in (prolitogenic) urinary calcium and a decrease in protective urinary citrate (via acidosis-mediated increased citrate reabsorption from the proximal tubule). In the case of dRTA, a third factor comes into play: alkaline urinary pH, which promotes calcium-phosphate precipitation and formation of calcium-phosphate-containing kidney stones (apatite stones). dRTA can be acquired or inherited. Acquired forms of dRTA occur with genetic diseases that affect tubular function (e.g., Wilson disease, hereditary fructose intolerance), hypercalciuric disorders (e.g., primary hyperparathyroidism, vitamin D intoxication), dysproteinemic syndromes (e.g., hypergammaglobulinemia, cryoglobulinemia, amyloidosis), autoimmune diseases (e.g.,

systemic lupus erythematosus, Sjögren's syndrome), and drugs/toxins (e.g., amphotericin B, lithium, pentamidine, vanadium) (140). Six monogenetic forms of dRTA are currently known: autosomal-recessive and autosomal-dominant mutations in anion exchanger 1 (AE1; encoded by *SLC4A1*), autosomal-recessive mutations in the B1 and a4 subunits of the V-ATPase (encoded by *ATP6V1B1* and *ATP6V0A4*, respectively), autosomal-recessive mutations in the transcription factor Forkhead Box I1 (Foxi1; encoded by *FOXI1*), autosomal-recessive mutations in tryptophan-aspartate repeat domain 72 (WDR72), and autosomal-recessive mutations in carbonic anhydrase type II (encoded by *CA2*) (141). *CA2* mutations cause a combined proximal-distal RTA, also known as type III RTA, but the renal phenotype is similar to that of isolated cases of inherited dRTA. Pharmacological carbonic anhydrase inhibition (e.g., topiramate, acetazolamide) causes systemic metabolic acidosis with a reduction in urinary citrate, a rise in urinary pH due to impaired tubular bicarbonate reabsorption, and a rise in urinary calcium excretion, thereby predisposing to calcium-phosphate stone formation (142).

FUTURE DIRECTIONS

To better understand and consequently design improved treatments for hypercalciuria and thereby prevent kidney stone formation, model systems are required. Current cell models employ renal tubular epithelial cells exposed to calcium-oxalate crystals. There are a variety of genetically modified mouse models with hypercalciuria. These include animals with hypercalciuria due to increased 1,25-dihydroxyvitamin D levels from hypophosphatemia, such as *Slc34a1* knockout mice, or due to deletion of a 1,25-dihydroxyvitamin D feedback inhibitor such as *FGF23* or *klotho* (104, 107), although the latter models are complicated by direct effects on renal calcium handling. As described above, mice with transgenic overexpression of *Trpv6* in the intestine display hypercalciuria due to increased intestinal calcium absorption (125). There are also many animal models of hypercalciuria due to defects in tubular reabsorption. Mice knocked out for *Nhe3*, *Cldn2*, and *Clc5* have hypercalciuria due, at least in part, to defective calcium reabsorption from the proximal tubule (37, 49, 143). *Cldn16*- and *Slc12a1*-deficient mice display defective calcium transport in the TAL, causing hypercalciuria (144–146). Finally, mice with deletion of *Trpv5* exhibit dramatic hypercalciuria (95).

Most of these models, however, do not develop renal calcifications, with the exception of *Abcc6*, *Slc34a1*, *Cldn2*, *klotho/fgf23*, and *Cldn10* knockout mice. Of these, only the *Abcc6* and *Cldn2* knockout mice demonstrate calcifications in the renal papillae, thereby resembling Randall plaques as seen in hypercalciuric kidney stone formers (49, 147). *Cldn2* knockout mice also display both a renal calcium leak in the proximal tubule and increased intestinal calcium absorption, consistent with the phenotype of many patients with hypercalciuria and calcium stones. This model therefore shows promise in furthering our understanding of the pathophysiology of calcium stone disease.

The genetic hypercalciuric stone-forming rat is another model that has contributed greatly to our understanding of hypercalciuria and kidney stone disease. This rat model has been specifically inbred to have increased urinary calcium excretion. The hypercalciuria is multifold and a result of increased intestinal calcium absorption, increased bone resorption, and reduced renal tubular reabsorption. The molecular etiology of these physiological alterations appears to be increased expression of the vitamin D receptor (VDR) at these sites (148). This is consistent with known associations between SNPs in *VDR* and kidney stone formation in some populations (149). Moreover, common interventions that reduce calciuria and kidney stone formation, including thiazide diuretics and a low-sodium diet (148, 150), are effective in this model system. The genetic hypercalciuric stone-forming rat is therefore an excellent model to test novel prevention therapies for stone formation. Given the absence of new therapies for the treatment of kidney stones, the

limited effectiveness of current therapies, and the large financial and health care costs associated with kidney stones, new therapies are greatly needed.

CONCLUSIONS

Kidney stones are common, painful, and costly. The greatest risk factor is increased urinary calcium excretion, which can occur due to increased intestinal absorption, increased bone resorption, or decreased renal reabsorption of calcium. Despite significant advances in our understanding of the molecular pathways conferring calcium homeostasis in the intestine, bone, and kidney and the creation of rodent models to study this, new therapies for calcium-based kidney stones have not been generated for decades. With further understanding of the underlying pathways that drive hypercalciuria and stone disease coupled with innovation, we hope this will be remedied in the coming years.

DISCLOSURE STATEMENT

R.T.A. has received consulting fees/honoraria from Ardylex, Ultragenyx, and Advicenne. D.G.F. has consulted for Otsuka Pharmaceuticals and Alnylam and has received unrestricted research funding from Novartis, Abbvie, Otsuka Pharmaceuticals, and Boehringer Ingelheim. H.D. is not aware of any affiliations, memberships, funding, or financial holdings that might be perceived as affecting the objectivity of this review.

ACKNOWLEDGMENTS

Owing to a strict reference limit, we were unable to include many primary sources and apologize for this omission. Research in the R.T.A. laboratory is funded by grants from the Women and Children's Health Research Institute, which is supported by the Stollery Children's Hospital Foundation, the Canadian Institutes of Health Research, the Kidney Foundation of Canada, and the National Sciences and Engineering Research Council of Canada. R.T.A. is a Stollery Science Laboratory Distinguished Researcher and the Canada Research Chair in Renal Epithelial Transport Physiology. D.G.F. is supported by the Swiss National Science Foundation (grants 31003A_152829, 3100A_172974, and 33IC30_166785) and the Swiss National Science Foundation–funded National Centers for Competence in Research (NCCR Transcure and NCCR Kidney.CH). H.D. is supported by the Novo Nordisk Foundation, the Carlsberg Foundation, and the Independent Research Fund Denmark.

LITERATURE CITED

1. Shoag J, Tasian GE, Goldfarb DS, Eisner BH. 2015. The new epidemiology of nephrolithiasis. *Adv. Chronic Kidney Dis.* 22:273–78
2. Canvasser NE, Alken P, Lipkin M, Nakada SY, Sodha HS, et al. 2017. The economics of stone disease. *World J. Urol.* 35:1321–29
3. Alexander RT, Hemmelgarn BR, Wiebe N, Bello A, Morgan C, et al. 2012. Kidney stones and kidney function loss: a cohort study. *BMJ* 345:e5287
4. Rule AD, Roger VL, Melton LJ 3rd, Bergstralh EJ, Li X, et al. 2010. Kidney stones associate with increased risk for myocardial infarction. *J. Am. Soc. Nephrol.* 21:1641–44
5. Taylor EN, Stampfer MJ, Curhan GC. 2005. Diabetes mellitus and the risk of nephrolithiasis. *Kidney Int.* 68:1230–35
6. Dimke H, Winther-Jensen M, Allin KH, Lund L, Jess T. 2021. Risk of urolithiasis in patients with inflammatory bowel disease: a nationwide Danish cohort study 1977–2018. *Clin. Gastroenterol. Hepatol.* 19:2532–40.e2

7. Alexander RT, Hemmelgarn BR, Wiebe N, Bello A, Samuel S, et al. 2014. Kidney stones and cardiovascular events: a cohort study. *Clin. J. Am. Soc. Nephrol.* 9:506–12
8. Ferraro PM, Taylor EN, Eisner BH, Gambaro G, Rimm EB, et al. 2013. History of kidney stones and the risk of coronary heart disease. *JAMA* 310:408–15
9. Knoll T, Schubert AB, Fahlenkamp D, Leusmann DB, Wendt-Nordahl G, Schubert G. 2011. Urolithiasis through the ages: data on more than 200,000 urinary stone analyses. *J. Urol.* 185:1304–11
10. Levy FL, Adams-Huet B, Pak CY. 1995. Ambulatory evaluation of nephrolithiasis: an update of a 1980 protocol. *Am. J. Med.* 98:50–59
11. Pak CY, Sakhaee K, Moe OW, Poindexter J, Adams-Huet B, et al. 2011. Defining hypercalciuria in nephrolithiasis. *Kidney Int.* 80:777–82
12. Pak CY, Kaplan R, Bone H, Townsend J, Waters O. 1975. A simple test for the diagnosis of absorptive, resorptive and renal hypercalciurias. *N. Engl. J. Med.* 292:497–500
13. Sakhaee K, Maalouf NM, Kumar R, Pasch A, Moe OW. 2011. Nephrolithiasis-associated bone disease: pathogenesis and treatment options. *Kidney Int.* 79:393–403
14. Shah A, Ramakrishnan S. 2020. Hyperoxaluria. In *StatPearls*. Treasure Island, FL: StatPearls Publ.
15. Witting C, Langman CB, Assimos D, Baum MA, Kausz A, et al. 2021. Pathophysiology and treatment of enteric hyperoxaluria. *Clin. J. Am. Soc. Nephrol.* 16(3):487–95
16. Leslie SW, Bashir K. 2021. Hypocitraturia and renal calculi. In *StatPearls*. Treasure Island, FL: StatPearls Publ.
17. Asplin JR, Parks JH, Coe FL. 1997. Dependence of upper limit of metastability on supersaturation in nephrolithiasis. *Kidney Int.* 52:1602–8
18. Parks JH, Coward M, Coe FL. 1997. Correspondence between stone composition and urine supersaturation in nephrolithiasis. *Kidney Int.* 51:894–900
19. Ferraro PM, Ticinesi A, Meschi T, Rodgers A, Di Maio F, et al. 2018. Short-term changes in urinary relative supersaturation predict recurrence of kidney stones: a tool to guide preventive measures in urolithiasis. *J. Urol.* 200:1082–87
20. Borghi L, Meschi T, Amato F, Briganti A, Novarini A, Giannini A. 1996. Urinary volume, water and recurrences in idiopathic calcium nephrolithiasis: a 5-year randomized prospective study. *J. Urol.* 155:839–43
21. Borghi L, Schianchi T, Meschi T, Guerra A, Allegri F, et al. 2002. Comparison of two diets for the prevention of recurrent stones in idiopathic hypercalciuria. *N. Engl. J. Med.* 346:77–84
22. Coe FL, Evan AP, Worcester EM, Lingeman JE. 2010. Three pathways for human kidney stone formation. *Urol. Res.* 38:147–60
23. Randall A. 1937. The origin and growth of renal calculi. *Ann. Surg.* 105:1009–27
24. Evan AP, Lingeman JE, Coe FL, Parks JH, Bledsoe SB, et al. 2003. Randall's plaque of patients with nephrolithiasis begins in basement membranes of thin loops of Henle. *J. Clin. Investig.* 111:607–16
25. Coe FL, Evan AP, Lingeman JE, Worcester EM. 2010. Plaque and deposits in nine human stone diseases. *Urol. Res.* 38:239–47
26. Worcester EM, Gillen DL, Evan AP, Parks JH, Wright K, et al. 2007. Evidence that postprandial reduction of renal calcium reabsorption mediates hypercalciuria of patients with calcium nephrolithiasis. *Am. J. Physiol. Ren. Physiol.* 292:F66–75
27. Alexander RT, Dimke H, Cordat E. 2013. Proximal tubular NHEs: sodium, protons and calcium? *Am. J. Physiol. Ren. Physiol.* 305:F229–36
28. Wright FS, Bomsztyk K. 1986. Calcium transport by the proximal tubule. *Adv. Exp. Med. Biol.* 208:165–70
29. Sutton RA, Walker VR. 1980. Responses to hydrochlorothiazide and acetazolamide in patients with calcium stones. Evidence suggesting a defect in renal tubular function. *N. Engl. J. Med.* 302:709–13
30. Worcester EM, Coe FL, Evan AP, Bergsland KJ, Parks JH, et al. 2008. Evidence for increased postprandial distal nephron calcium delivery in hypercalciuric stone-forming patients. *Am. J. Physiol. Ren. Physiol.* 295:F1286–94
31. Bello-Reuss E. 1986. Cell membranes and paracellular resistances in isolated renal proximal tubules from rabbit and Ambystoma. *J. Physiol.* 370:25–38

32. Plain A, Pan W, O'Neill D, Ure M, Beggs MR, et al. 2020. Claudin-12 knockout mice demonstrate reduced proximal tubule calcium permeability. *Int. J. Mol. Sci.* 21:2074
33. Sutton RA, Dirks JH. 1975. The renal excretion of calcium: a review of micropuncture data. *Can. J. Physiol. Pharmacol.* 53:979–88
34. Alexander RT, Rievaj J, Dimke H. 2014. Paracellular calcium transport across renal and intestinal epithelia. *Biochem. Cell Biol.* 92:467–80
35. Edwards A, Bonny O. 2018. A model of calcium transport and regulation in the proximal tubule. *Am. J. Physiol. Ren. Physiol.* 315:F942–53
36. Schultheis PJ, Clarke LL, Meneton P, Miller ML, Soleimani M, et al. 1998. Renal and intestinal absorptive defects in mice lacking the NHE3 Na^+/H^+ exchanger. *Nat. Genet.* 19:282–85
37. Pan W, Borovac J, Spicer Z, Hoenderop JG, Bindels RJ, et al. 2012. The epithelial sodium/proton exchanger, NHE3, is necessary for renal and intestinal calcium (re)absorption. *Am. J. Physiol. Ren. Physiol.* 302:F943–56
38. Janecke AR, Heinz-Erian P, Yin J, Petersen BS, Franke A, et al. 2015. Reduced sodium/proton exchanger NHE3 activity causes congenital sodium diarrhea. *Hum. Mol. Genet.* 24:6614–23
39. Rievaj J, Pan W, Cordat E, Alexander RT. 2013. The Na^+/H^+ exchanger isoform 3 is required for active paracellular and transcellular Ca^{2+} transport across murine cecum. *Am. J. Physiol. Gastrointest. Liver Physiol.* 305:G303–13
40. Wiebe SA, Plain A, Pan W, O'Neill D, Braam B, Alexander RT. 2019. NHE8 attenuates Ca^{2+} influx into NRK cells and the proximal tubule epithelium. *Am. J. Physiol. Ren. Physiol.* 317:F240–53
41. Blau JE, Bauman V, Conway EM, Piaggi P, Walter MF, et al. 2018. Canagliflozin triggers the FGF23/1,25-dihydroxyvitamin D/PTH axis in healthy volunteers in a randomized crossover study. *JCI Insight* 3:e99123
42. Schneider D, Gauthier B, Trachtman H. 1992. Hypercalciuria in children with renal glycosuria: evidence of dual renal tubular reabsorptive defects. *J. Pediatr.* 121:715–19
43. Schnermann J, Chou CL, Ma T, Traynor T, Knepper MA, Verkman AS. 1998. Defective proximal tubular fluid reabsorption in transgenic aquaporin-1 null mice. *PNAS* 95:9660–64
44. Sabolic I, Valenti G, Verbavatz JM, Van Hoek AN, Verkman AS, et al. 1992. Localization of the CHIP28 water channel in rat kidney. *Am. J. Physiol.* 263:C1225–33
45. Urabe Y, Tanikawa C, Takahashi A, Okada Y, Morizono T, et al. 2012. A genome-wide association study of nephrolithiasis in the Japanese population identifies novel susceptible loci at 5q35.3, 7p14.3, and 13q14.1. *PLOS Genet.* 8:e1002541
46. Barratt LJ, Rector FC Jr., Kokko JP, Seldin DW. 1974. Factors governing the transepithelial potential difference across the proximal tubule of the rat kidney. *J. Clin. Investig.* 53:454–64
47. Balkovetz DF. 2006. Claudins at the gate: determinants of renal epithelial tight junction paracellular permeability. *Am. J. Physiol. Ren. Physiol.* 290:F572–79
48. Kiuchi-Saishin Y, Gotoh S, Furuse M, Takasuga A, Tano Y, Tsukita S. 2002. Differential expression patterns of claudins, tight junction membrane proteins, in mouse nephron segments. *J. Am. Soc. Nephrol.* 13:875–86
49. Curry JN, Saurette M, Askari M, Pei L, Filla MB, et al. 2020. Claudin-2 deficiency associates with hypercalciuria in mice and human kidney stone disease. *J. Clin. Investig.* 130:1948–60
50. Enck AH, Berger UV, Yu AS. 2001. Claudin-2 is selectively expressed in proximal nephron in mouse kidney. *Am. J. Physiol. Ren. Physiol.* 281:F966–74
51. Schlingmann KP, Kaufmann M, Weber S, Irwin A, Goos C, et al. 2011. Mutations in CYP24A1 and idiopathic infantile hypercalcemia. *N. Engl. J. Med.* 365:410–21
52. Schlingmann KP, Ruminska J, Kaufmann M, Dursun I, Patti M, et al. 2016. Autosomal-recessive mutations in *SLC34A1* encoding sodium-phosphate cotransporter 2A cause idiopathic infantile hypercalcemia. *J. Am. Soc. Nephrol.* 27:604–14
53. Bergwitz C, Roslin NM, Tieder M, Loredo-Osti JC, Bastepe M, et al. 2006. *SLC34A3* mutations in patients with hereditary hypophosphatemic rickets with hypercalciuria predict a key role for the sodium-phosphate cotransporter NaP_i-IIc in maintaining phosphate homeostasis. *Am. J. Hum. Genet.* 78:179–92
54. Alexander RT, Dimke H. 2017. Effect of diuretics on renal tubular transport of calcium and magnesium. *Am. J. Physiol. Ren. Physiol.* 312:F998–1015

55. Parfitt AM. 1969. Acetazolamide and sodium bicarbonate induced nephrocalcinosis and nephrolithiasis; relationship to citrate and calcium excretion. *Arch. Intern. Med.* 124:736–40
56. Suki WN. 1979. Calcium transport in the nephron. *Am. J. Physiol.* 237:F1–6
57. Di Stefano A, Roinel N, de Rouffignac C, Wittner M. 1993. Transepithelial Ca^{2+} and Mg^{2+} transport in the cortical thick ascending limb of Henle's loop of the mouse is a voltage-dependent process. *Ren. Physiol. Biochem.* 16:157–66
58. Simon DB, Karet FE, Hamdan JM, DiPietro A, Sanjad SA, Lifton RP. 1996. Bartter's syndrome, hypokalaemic alkalosis with hypercalciuria, is caused by mutations in the Na-K-2Cl cotransporter NKCC2. *Nat. Genet.* 13:183–88
59. Greger R, Schlatter E. 1983. Properties of the lumen membrane of the cortical thick ascending limb of Henle's loop of rabbit kidney. *Pflugers Arch.* 396:315–24
60. Dimke H, Schnermann J. 2018. Axial and cellular heterogeneity in electrolyte transport pathways along the thick ascending limb. *Acta Physiol.* 223:e13057
61. Simon DB, Karet FE, Rodriguez-Soriano J, Hamdan JH, DiPietro A, et al. 1996. Genetic heterogeneity of Bartter's syndrome revealed by mutations in the K^+ channel, ROMK. *Nat. Genet.* 14:152–56
62. Pope JC 4th, Trusler LA, Klein AM, Walsh WF, Yared A, Brock JW 3rd. 1996. The natural history of nephrocalcinosis in premature infants treated with loop diuretics. *J. Urol.* 156(2 Pt. 2):709–12
63. Simon DB, Bindra RS, Mansfield TA, Nelson-Williams C, Mendonca E, et al. 1997. Mutations in the chloride channel gene, *CLCNKB*, cause Bartter's syndrome type III. *Nat. Genet.* 17:171–78
64. McCredie DA, Rotenberg E, Williams AL. 1974. Hypercalciuria in potassium-losing nephropathy: a variant of Bartter's syndrome. *Aust. Paediatr. J.* 10:286–95
65. Laghmani K, Beck BB, Yang SS, Seaayfan E, Wenzel A, et al. 2016. Polyhydramnios, transient antenatal Bartter's syndrome, and *MAGED2* mutations. *N. Engl. J. Med.* 374:1853–63
66. Di Stefano A, Wittner M, Nitschke R, Braitsch R, Greger R, et al. 1990. Effects of parathyroid hormone and calcitonin on Na^+, Cl^-, K^+, Mg^{2+} and Ca^{2+} transport in cortical and medullary thick ascending limbs of mouse kidney. *Pflugers Arch.* 417:161–67
67. Milatz S, Himmerkus N, Wulfmeyer VC, Drewell H, Mutig K, et al. 2016. Mosaic expression of claudins in thick ascending limbs of Henle results in spatial separation of paracellular Na^+ and Mg^{2+} transport. *PNAS* 114(2):E219–27
68. Simon DB, Lu Y, Choate KA, Velazquez H, Al-Sabban E, et al. 1999. Paracellin-1, a renal tight junction protein required for paracellular Mg^{2+} resorption. *Science* 285:103–6
69. Konrad M, Schaller A, Seelow D, Pandey AV, Waldegger S, et al. 2006. Mutations in the tight-junction gene claudin 19 (*CLDN19*) are associated with renal magnesium wasting, renal failure, and severe ocular involvement. *Am. J. Hum. Genet.* 79:949–57
70. Praga M, Vara J, Gonzalez-Parra E, Andres A, Alamo C, et al. 1995. Familial hypomagnesemia with hypercalciuria and nephrocalcinosis. *Kidney Int.* 47:1419–25
71. Will C, Breiderhoff T, Thumfart J, Stuiver M, Kopplin K, et al. 2010. Targeted deletion of murine *Cldn16* identifies extra- and intrarenal compensatory mechanisms of Ca^{2+} and Mg^{2+} wasting. *Am. J. Physiol. Ren. Physiol.* 298:F1152–61
72. Hou J, Renigunta A, Konrad M, Gomes AS, Schneeberger EE, et al. 2008. Claudin-16 and claudin-19 interact and form a cation-selective tight junction complex. *J. Clin. Investig.* 118:619–28
73. Muto Y, Wilson PC, Ledru N, Wu H, Dimke H, et al. 2021. Single cell transcriptional and chromatin accessibility profiling redefine cellular heterogeneity in the adult human kidney. *Nat. Commun.* 12:2190
74. Chen L, Chou CL, Knepper MA. 2021. Targeted single-cell RNA-seq identifies minority cell types of kidney distal nephron. *J. Am. Soc. Nephrol.* 32:886–96
75. Breiderhoff T, Himmerkus N, Stuiver M, Mutig K, Will C, et al. 2012. Deletion of *claudin-10* (*Cldn10*) in the thick ascending limb impairs paracellular sodium permeability and leads to hypermagnesemia and nephrocalcinosis. *PNAS* 109:14241–46
76. Breiderhoff T, Himmerkus N, Drewell H, Plain A, Gunzel D, et al. 2018. Deletion of claudin-10 rescues claudin-16-deficient mice from hypomagnesemia and hypercalciuria. *Kidney Int.* 93:580–88
77. Wittner M, Mandon B, Roinel N, de Rouffignac C, Di Stefano A. 1993. Hormonal stimulation of Ca^{2+} and Mg^{2+} transport in the cortical thick ascending limb of Henle's loop of the mouse: evidence for a change in the paracellular pathway permeability. *Pflugers Arch.* 423:387–96

78. Ikari A, Matsumoto S, Harada H, Takagi K, Hayashi H, et al. 2006. Phosphorylation of paracellin-1 at Ser217 by protein kinase A is essential for localization in tight junctions. *J. Cell Sci.* 119:1781–89
79. Desfleurs E, Wittner M, Simeone S, Pajaud S, Moine G, et al. 1998. Calcium-sensing receptor: regulation of electrolyte transport in the thick ascending limb of Henle's loop. *Kidney Blood Press. Res.* 21:401–12
80. Loupy A, Ramakrishnan SK, Wootla B, Chambrey R, de la Faille R, et al. 2012. PTH-independent regulation of blood calcium concentration by the calcium-sensing receptor. *J. Clin. Investig.* 122:3355–67
81. Dimke H, Desai P, Borovac J, Lau A, Pan W, Alexander RT. 2013. Activation of the Ca^{2+}-sensing receptor increases renal claudin-14 expression and urinary Ca^{2+} excretion. *Am. J. Physiol. Ren. Physiol.* 304(6):F761–69
82. Gong Y, Hou J. 2014. Claudin-14 underlies Ca^{++}-sensing receptor-mediated Ca^{++} metabolism via NFAT-microRNA-based mechanisms. *J. Am. Soc. Nephrol.* 25(4):745–60
83. Gong Y, Renigunta V, Himmerkus N, Zhang J, Renigunta A, et al. 2012. Claudin-14 regulates renal Ca^{++} transport in response to CaSR signalling via a novel microRNA pathway. *EMBO J.* 31(8):1999–2012
84. Frische S, Alexander RT, Ferreira P, Siu Ga Tan R, Wang W, et al. 2021. Localization and regulation of claudin-14 in experimental models of hypercalcemia. *Am. J. Physiol. Ren. Physiol.* 320(1):F74–86
85. Plain A, Wulfmeyer VC, Milatz S, Klietz A, Hou J, et al. 2016. Corticomedullary difference in the effects of dietary Ca^{2+} on tight junction properties in thick ascending limbs of Henle's loop. *Pflugers Arch.* 468:293–303
86. Wilcox ER, Burton QL, Naz S, Riazuddin S, Smith TN, et al. 2001. Mutations in the gene encoding tight junction claudin-14 cause autosomal recessive deafness *DFNB29*. *Cell* 104:165–72
87. Ben-Yosef T, Belyantseva IA, Saunders TL, Hughes ED, Kawamoto K, et al. 2003. Claudin 14 knockout mice, a model for autosomal recessive deafness *DFNB29*, are deaf due to cochlear hair cell degeneration. *Hum. Mol. Genet.* 12:2049–61
88. Dimke H, Hoenderop JG, Bindels RJ. 2009. Hereditary tubular transport disorders: implications for renal handling of Ca^{2+} and Mg^{2+}. *Clin. Sci.* 118:1–18
89. Obermüller N, Bernstein P, Velázquez H, Reilly R, Moser D, et al. 1995. Expression of the thiazide-sensitive Na-Cl cotransporter in rat and human kidney. *Am. J. Physiol.* 269:F900–10
90. Lassiter WE, Gottschalk CW, Mylle M. 1963. Micropuncture study of renal tubular reabsorption of calcium in normal rodents. *Am. J. Physiol.* 204:771–75
91. Hoenderop JG, van der Kemp AW, Hartog A, van de Graaf SF, van Os CH, et al. 1999. Molecular identification of the apical Ca^{2+} channel in 1,25-dihydroxyvitamin D_3-responsive epithelia. *J. Biol. Chem.* 274:8375–78
92. Koster HP, Hartog A, van Os CH, Bindels RJ. 1995. Calbindin-D28K facilitates cytosolic calcium diffusion without interfering with calcium signaling. *Cell Calcium* 18:187–96
93. Reilly RF, Shugrue CA, Lattanzi D, Biemesderfer D. 1993. Immunolocalization of the Na^+/Ca^{2+} exchanger in rabbit kidney. *Am. J. Physiol.* 265:F327–32
94. Alexander RT, Beggs MR, Zamani R, Marcussen N, Frische S, Dimke H. 2015. Ultrastructural and immunohistochemical localization of plasma membrane Ca^{2+}-ATPase 4 in Ca^{2+}-transporting epithelia. *Am. J. Physiol. Ren. Physiol.* 309:F604–16
95. Hoenderop JG, van Leeuwen JP, van der Eerden BC, Kersten FF, van der Kemp AW, et al. 2003. Renal Ca^{2+} wasting, hyperabsorption, and reduced bone thickness in mice lacking TRPV5. *J. Clin. Investig.* 112:1906–14
96. Oddsson A, Sulem P, Helgason H, Edvardsson VO, Thorleifsson G, et al. 2015. Common and rare variants associated with kidney stones and biochemical traits. *Nat. Commun.* 6:7975
97. Hoenderop JG, Müller D, van der Kemp AW, Hartog A, Suzuki M, et al. 2001. Calcitriol controls the epithelial calcium channel in kidney. *J. Am. Soc. Nephrol.* 12:1342–49
98. van Abel M, Hoenderop JG, van der Kemp AW, Friedlaender MM, van Leeuwen JP, Bindels RJ. 2005. Coordinated control of renal Ca^{2+} transport proteins by parathyroid hormone. *Kidney Int.* 68:1708–21
99. Bailly C, Roinel N, Amiel C. 1985. Stimulation by glucagon and PTH of Ca and Mg reabsorption in the superficial distal tubule of the rat kidney. *Pflugers Arch.* 403:28–34

100. de Groot T, Lee K, Langeslag M, Xi Q, Jalink K, et al. 2009. Parathyroid hormone activates TRPV5 via PKA-dependent phosphorylation. *J. Am. Soc. Nephrol.* 20:1693–704
101. Cha SK, Wu T, Huang CL. 2008. Protein kinase C inhibits caveolae-mediated endocytosis of TRPV5. *Am. J. Physiol. Ren. Physiol.* 294:F1212–21
102. Hsu YJ, Dimke H, Schoeber JP, Hsu SC, Lin SH, et al. 2010. Testosterone increases urinary calcium excretion and inhibits expression of renal calcium transport proteins. *Kidney Int.* 77:601–8
103. Alexander RT, Cordat E, Chambrey R, Dimke H, Eladari D. 2016. Acidosis and urinary calcium excretion: insights from genetic disorders. *J. Am. Soc. Nephrol.* 27:3511–20
104. Alexander RT, Woudenberg-Vrenken TE, Buurman J, Dijkman H, van der Eerden BC, et al. 2009. Klotho prevents renal calcium loss. *J. Am. Soc. Nephrol.* 20:2371–79
105. Chang Q, Hoefs S, van der Kemp AW, Topala CN, Bindels RJ, Hoenderop JG. 2005. The β-glucuronidase klotho hydrolyzes and activates the TRPV5 channel. *Science* 310:490–93
106. Chen G, Liu Y, Goetz R, Fu L, Jayaraman S, et al. 2018. α-Klotho is a non-enzymatic molecular scaffold for FGF23 hormone signalling. *Nature* 553:461–66
107. Andrukhova O, Smorodchenko A, Egerbacher M, Streicher C, Zeitz U, et al. 2014. FGF23 promotes renal calcium reabsorption through the TRPV5 channel. *EMBO J.* 33:229–46
108. Laerum E, Larsen S. 1984. Thiazide prophylaxis of urolithiasis. A double-blind study in general practice. *Acta Med. Scand.* 215:383–89
109. Brickman AS, Massry SG, Coburn JW. 1972. Changes in serum and urinary calcium during treatment with hydrochlorothiazide: studies on mechanisms. *J. Clin. Investig.* 51:945–54
110. Gitelman HJ, Graham JB, Welt LG. 1966. A new familial disorder characterized by hypokalemia and hypomagnesemia. *Trans. Assoc. Am. Physicians* 79:221–35
111. Reilly RF, Huang CL. 2011. The mechanism of hypocalciuria with NaCl cotransporter inhibition. *Nat. Rev. Nephrol.* 7:669–74
112. Loffing J, Vallon V, Loffing-Cueni D, Aregger F, Richter K, et al. 2004. Altered renal distal tubule structure and renal Na^+ and Ca^{2+} handling in a mouse model for Gitelman's syndrome. *J. Am. Soc. Nephrol.* 15:2276–88
113. Schultheis PJ, Lorenz JN, Meneton P, Nieman ML, Riddle TM, et al. 1998. Phenotype resembling Gitelman's syndrome in mice lacking the apical Na^+-Cl^- cotransporter of the distal convoluted tubule. *J. Biol. Chem.* 273:29150–55
114. Nijenhuis T, Vallon V, van der Kemp AW, Loffing J, Hoenderop JG, Bindels RJ. 2005. Enhanced passive Ca^{2+} reabsorption and reduced Mg^{2+} channel abundance explains thiazide-induced hypocalciuria and hypomagnesemia. *J. Clin. Investig.* 115:1651–58
115. Lee JJ, Liu X, O'Neill D, Beggs MR, Weissgerber P, et al. 2019. Activation of the calcium sensing receptor attenuates TRPV6-dependent intestinal calcium absorption. *JCI Insight* 5(11):e128013
116. Pak CY, Britton F, Peterson R, Ward D, Northcutt C, et al. 1980. Ambulatory evaluation of nephrolithiasis. Classification, clinical presentation and diagnostic criteria. *Am. J. Med.* 69:19–30
117. Beggs MR, Alexander RT. 2017. Intestinal absorption and renal reabsorption of calcium throughout postnatal development. *Exp. Biol. Med.* 242:840–49
118. Bianco SDC, Peng J-B, Takanaga H, Suzuki Y, Crescenzi A, et al. 2007. Marked disturbance of calcium homeostasis in mice with targeted disruption of the *Trpv6* calcium channel gene. *J. Bone Miner. Res.* 22:274–85
119. Woudenberg-Vrenken TE, Lameris AL, Weißgerber P, Olausson J, Flockerzi V, et al. 2012. Functional TRPV6 channels are crucial for transepithelial Ca^{2+} absorption. *Am. J. Physiol. Gastrointest. Liver Physiol.* 303:G879–85
120. Reyes-Fernandez PC, Fleet JC. 2015. Luminal glucose does not enhance active intestinal calcium absorption in mice: evidence against a role for $Ca_v1.3$ as a mediator of calcium uptake during absorption. *Nutr. Res.* 35:1009–15
121. Morgan EL, Mace OJ, Affleck J, Kellett GL. 2007. Apical GLUT2 and $Ca_v1.3$: regulation of rat intestinal glucose and calcium absorption. *J. Physiol.* 580:593–604
122. Beggs MR, Lee JJ, Busch K, Raza A, Dimke H, et al. 2019. TRPV6 and $Ca_v1.3$ mediate distal small intestine calcium absorption before weaning. *Cell Mol. Gastroenterol. Hepatol.* 8:625–42

123. Mittermeier L, Demirkhanyan L, Stadlbauer B, Breit A, Recordati C, et al. 2019. TRPM7 is the central gatekeeper of intestinal mineral absorption essential for postnatal survival. *PNAS* 116:4706–15
124. van Abel M, Hoenderop JG, van der Kemp AW, van Leeuwen JP, Bindels RJ. 2003. Regulation of the epithelial Ca^{2+} channels in small intestine as studied by quantitative mRNA detection. *Am. J. Physiol. Gastrointest. Liver Physiol.* 285:G78–85
125. Cui M, Li Q, Johnson R, Fleet JC. 2012. Villin promoter-mediated transgenic expression of transient receptor potential cation channel, subfamily V, member 6 (TRPV6) increases intestinal calcium absorption in wild-type and vitamin D receptor knockout mice. *J. Bone Miner. Res.* 27:2097–107
126. Suzuki Y, Pasch A, Bonny O, Mohaupt MG, Hediger MA, Frey FJ. 2008. Gain-of-function haplotype in the epithelial calcium channel TRPV6 is a risk factor for renal calcium stone formation. *Hum. Mol. Genet.* 17:1613–18
127. Fujita H, Sugimoto K, Inatomi S, Maeda T, Osanai M, et al. 2008. Tight junction proteins claudin-2 and -12 are critical for vitamin D-dependent Ca^{2+} absorption between enterocytes. *Mol. Biol. Cell* 19:1912–21
128. Duflos C, Bellaton C, Pansu D, Bronner F. 1995. Calcium solubility, intestinal sojourn time and paracellular permeability codetermine passive calcium absorption in rats. *J. Nutr.* 125:2348–55
129. Karbach U, Rummel W. 1987. Calcium transport across the colon ascendens and the influence of 1,25-dihydroxyvitamin D_3 and dexamethasone. *Eur. J. Clin. Investig.* 17:368–74
130. Mineo H, Hara H, Tomita F. 2001. Short-chain fatty acids enhance diffusional Ca transport in the epithelium of the rat cecum and colon. *Life Sci.* 69:517–26
131. Maierhofer WJ, Gray RW, Cheung HS, Lemann J Jr. 1983. Bone resorption stimulated by elevated serum 1,25-$(OH)_2$-vitamin D concentrations in healthy men. *Kidney Int.* 24:555–60
132. Coe FL, Parks JH. 1994. Idiopathic hypercalciuria: the contribution of Dr. Jacob Lemann, Jr. *J. Am. Soc. Nephrol.* 5:S59–69
133. Bleich HL, Moore MJ, Lemann J Jr., Adams ND, Gray RW. 1979. Urinary calcium excretion in human beings. *N. Engl. J. Med.* 301:535–41
134. Krieger NS, Frick KK, Bushinsky DA. 2004. Mechanism of acid-induced bone resorption. *Curr. Opin. Nephrol. Hypertens.* 13:423–36
135. Houillier P, Normand M, Froissart M, Blanchard A, Jungers P, Paillard M. 1996. Calciuric response to an acute acid load in healthy subjects and hypercalciuric calcium stone formers. *Kidney Int.* 50:987–97
136. Adams ND, Gray RW, Lemann J Jr. 1979. The calciuria of increased fixed acid production in humans: evidence against a role for parathyroid hormone and 1,25$(OH)_2$-vitamin D. *Calcif. Tissue Int.* 28:233–38
137. Sutton RA, Wong NL, Dirks JH. 1979. Effects of metabolic acidosis and alkalosis on sodium and calcium transport in the dog kidney. *Kidney Int.* 15:520–33
138. Yeh BI, Sun TJ, Lee JZ, Chen HH, Huang CL. 2003. Mechanism and molecular determinant for regulation of rabbit transient receptor potential type 5 (TRPV5) channel by extracellular pH. *J. Biol. Chem.* 278:51044–52
139. Nijenhuis T, Renkema KY, Hoenderop JG, Bindels RJ. 2006. Acid-base status determines the renal expression of Ca^{2+} and Mg^{2+} transport proteins. *J. Am. Soc. Nephrol.* 17:617–26
140. Rodríguez Soriano J. 2002. Renal tubular acidosis: the clinical entity. *J. Am. Soc. Nephrol.* 13:2160–70
141. Alexander RT, Law L, Gil-Peña H, Greenbaum LA, Santos F. 1993. Hereditary distal renal tubular acidosis. In *GeneReviews®*, ed. MP Adam, HH Ardinger, RA Pagon, SE Wallace, LJH Bean, et al. Seattle: Univ. Wash. Press
142. Welch BJ, Graybeal D, Moe OW, Maalouf NM, Sakhaee K. 2006. Biochemical and stone-risk profiles with topiramate treatment. *Am. J. Kidney Dis.* 48:555–63
143. Cebotaru V, Kaul S, Devuyst O, Cai H, Racusen L, et al. 2005. High citrate diet delays progression of renal insufficiency in the ClC-5 knockout mouse model of Dent's disease. *Kidney Int.* 68:642–52
144. Himmerkus N, Shan Q, Goerke B, Hou J, Goodenough DA, Bleich M. 2008. Salt and acid-base metabolism in claudin-16 knockdown mice: impact for the pathophysiology of FHHNC patients. *Am. J. Physiol. Ren. Physiol.* 295:F1641–47
145. Hou J, Shan Q, Wang T, Gomes AS, Yan Q, et al. 2007. Transgenic RNAi depletion of claudin-16 and the renal handling of magnesium. *J. Biol. Chem.* 282:17114–22

146. Takahashi N, Chernavvsky DR, Gomez RA, Igarashi P, Gitelman HJ, Smithies O. 2000. Uncompensated polyuria in a mouse model of Bartter's syndrome. *PNAS* 97:5434–39
147. Bouderlique E, Tang E, Perez J, Coudert A, Bazin D, et al. 2019. Vitamin D and calcium supplementation accelerates Randall's plaque formation in a murine model. *Am. J. Pathol.* 189:2171–80
148. Frick KK, Krieger NS, Bushinsky DA. 2015. Modeling hypercalciuria in the genetic hypercalciuric stone-forming rat. *Curr. Opin. Nephrol. Hypertens.* 24:336–44
149. Scott P, Ouimet D, Valiquette L, Guay G, Proulx Y, et al. 1999. Suggestive evidence for a susceptibility gene near the vitamin D receptor locus in idiopathic calcium stone formation. *J. Am. Soc. Nephrol.* 10:1007–13
150. Krieger NS, Asplin J, Granja I, Chen L, Spataru D, et al. 2021. Chlorthalidone with potassium citrate decreases calcium oxalate stones and increases bone quality in genetic hypercalciuric stone-forming rats. *Kidney Int.* 99(5):1118–26